

Intramolecular Energy Transfer and Predissociation in C-State HCN

D. T. CHULJIAN, J. OZMENT, and J. SIMONS

Chemistry Department, University of Utah, Salt Lake City, Utah 84112

Abstract

Using our *ab initio* configuration interaction potential energy surface for the C state of HCN, we carried out classical trajectory calculations aimed at simulating the predissociation dynamics of various vibronic states of HCN and DCN. Our results provide an interpretation of the experimental photofragment excitation spectrum of this species. They also indicate that tunneling, which had been postulated as a rate-determining step in the predissociation, is not substantial. Intramolecular energy transfer seems to be the slow step. Finally, there is evidence that on a time scale up to one rotational period, the predissociation kinetics is quite mode specific.

1. Introduction

An interpretation of the photofragment excitation (PFE) spectrum [1] of C-state HCN has recently been put forth by our laboratory [2]. Our interpretation was based on analysis of the experimental data together with an *ab initio* configuration interaction (CI) C-state potential energy surface which we computed at more than 150 different HCN geometries (with the CN bond length frozen). In this article we supplement this analysis via classical trajectory calculations in an attempt to achieve a more quantitative understanding of the rate and mechanism of predissociation of the various vibronic levels* (ν_1, ν_2) in the C-state HCN. Because our desire is to address the predissociation of only those vibronic states that do not involve excitation of the CN stretching mode, we have not included the r_{CN} degree of freedom in our potential surface. For situations in which large amounts of energy reside in the CH stretching or HCN bending modes, it is certainly likely that energy could flow into the CN mode. However, even in such cases, our desire to study only the $\nu_3 = 0$ lines in the PFE spectrum allows us to restrict r_{CN} in computing our energy surface.

In the PFE experiment of MacPherson and Simons [1] (MS), light in the wavelength range 130–155 nm is used to excite (linear) $X^1\Sigma$ HCN to various vibronic levels (ν_1, ν_2) of the C^1A' state. The intensity and polarization of the fluorescence of the $B^2\Sigma^+$ excited CN (produced by fragmentation of C-state

* The C-state's CH stretching vibration frequency (labeled with quantum number ν_1) is approximately 2300 cm^{-1} ; the bending frequency (labeled ν_2) is approximately 800 cm^{-1} . For the DCN isotope, which MS also studied, the respective frequencies are 1450 and 650 cm^{-1} . In generating the CI potential surface, we froze the CN distance because we were interested in interpreting only those lines in the PFE spectrum arising from ν_1, ν_2 excitation.

HCN: $\text{HCN}^* \rightarrow \text{H} + \text{CN}^*$, $\text{CN}^* \rightarrow \text{CN} + h\nu$) are monitored as functions of ν_1 and ν_2 . If no CN fluorescence is observed, it is inferred that the $\nu_1\nu_2$ level is bound (i.e., not dissociative). CN fluorescence that retains the polarization* of the exciting light is said to arise from dissociation of the $\nu_1\nu_2$ level that took place before the HCN had time to undergo several rotations ($\tau_{\text{rot}} \sim 2 \times 10^{-13}$ s). Fluorescence that has lost much of the initial polarization content arose from a level $\nu_1\nu_2$ that took longer* than τ_{rot} to dissociate. If the lines in the absorption or PFE spectrum display broadening comparable to the spacing between the vibrational lines of the bending progression ($\Delta\bar{\nu} \sim 800 \text{ cm}^{-1}$, which corresponds to $\Delta\lambda \approx 2 \text{ nm}$, near 135 nm), the dissociation is postulated to occur within approximately one bending vibration ($\tau_{\text{bend}} \sim 4 \times 10^{-14}$ s). Complete absence of vibrational structure in the PFE spectrum is interpreted to be due to *direct* dissociation of that $\nu_1\nu_2$ level.

By thus combining the polarization information with any broadening of the absorption or PFE spectrum, MS are able to place bounds on the rates of dissociation of various $\nu_1\nu_2$ levels of both HCN and DCN (whose rotation and bending times are $\sim 2 \times 10^{-13}$ and 5×10^{-14} s, respectively).

2. Rationalization of Experimental Data

Our *ab initio* CI potential energy surface for C-state HCN is displayed pictorially in Figure 1 and is described more quantitatively in ref. 2. Near the equilibrium bond angle (ca. 140°) of the HCN C state, the surface shows no barrier as a function of the radial coordinate.[†] Hence for very low values of the bending quantum number (ν_2), which correspond to HCN bond angles near 140° , we expect the various ν_1 levels to be either bound (if they lie below the dissociation threshold) or directly dissociative. However, as ν_2 increases, the molecule samples a wider region of bond angles. At angles greater than 150° or less than 125° , the C-state surface displays barriers[‡] along the radial coordinate (see Fig. 1). However, the depth of the potential energy well of this surface is reduced as the HCN angle deviates from 140° . As a result, we expect excitation of the ν_2 bending mode to have two effects. First, the appearance of a radial barrier should permit motion along the ν_1 stretching mode to become trapped (behind the barrier), thereby giving rise to a level (ν_1, ν_2) that could persist for a few vibrational periods. Second, the decrease in the depth of the well as ν_2 is excited (i.e., angular deviation increases) might be expected to allow the ν_1 mode's energy to move above the potential energy barrier. There is a competition between the tendency of the barrier to grow and the well to become more shallow as ν_2 increases. This should give rise to a region of ν_2 values corresponding to

* The fluorescence lifetime of the $B^2\Sigma^+$ CN radical is short enough so that CN rotation after HCN (DCN) fragmentation cannot be the major cause of depolarization.

† The radial coordinate r is measured from the center of mass of the CN moiety. This choice was made to facilitate treatment of the classical equations of motion. The HCN angular coordinate (θ) is defined to be 180° at the linear HCN geometry.

‡ As discussed in ref. 2, these barriers are due to avoided configuration crossings. They are not simply angular momentum barriers.

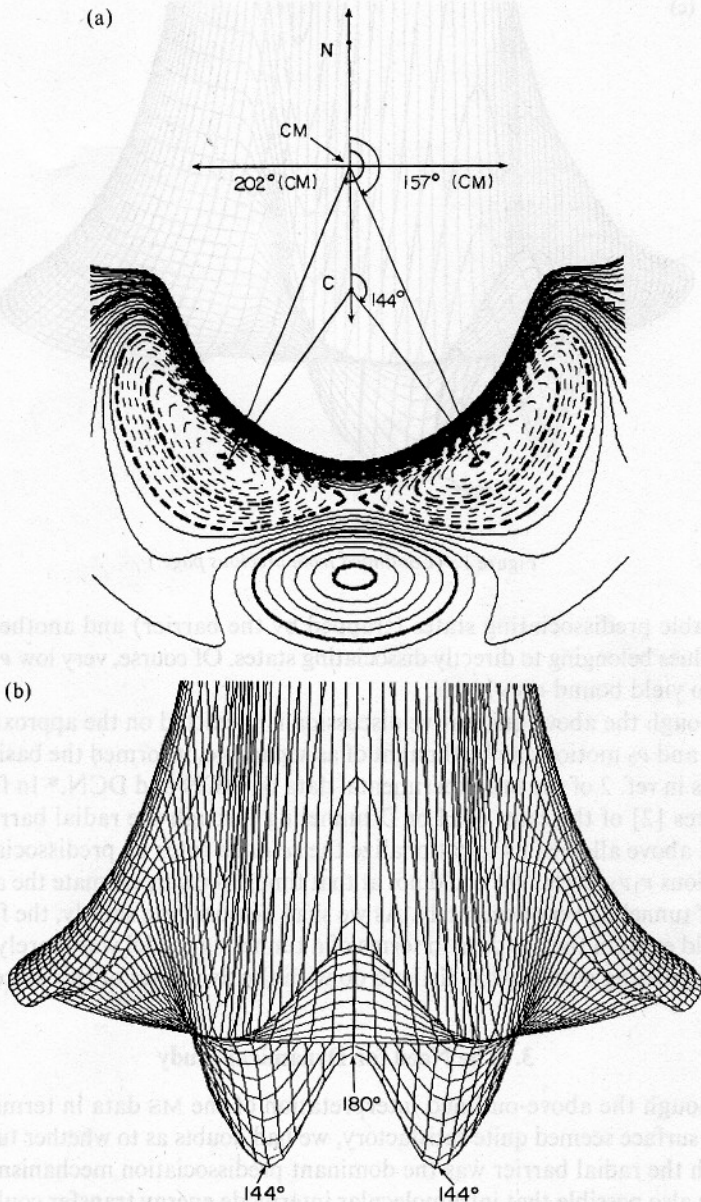


Figure 1. (a) The contour plot of the potential energy surface for C-state HCN. The energy ranges from -92.600 to -92.645 a.u. The HCN bond angle for the minimum of either energy well occurs at 144° (as labeled), at an H—C distance of 2.2 a.u. The two minima are shown here on a center of mass polar coordinate grid at $r = 3.3$ a.u. (CM) and $\theta = 157^\circ$ (CM) and $\theta = 203^\circ$ (CM). (b) The three-dimensional plot of the same surface as viewed along the C—N bond axis (180°). The minimum of the energy well at 144° are labeled as reference. (c) The same surface as viewed from $\theta = 140^\circ$ (CM). It shows the ridges that form the radial barrier at bond angles greater than 150° and less than 125° , as labeled. The 180° bond angle and the 144° bond angle are labeled as references.

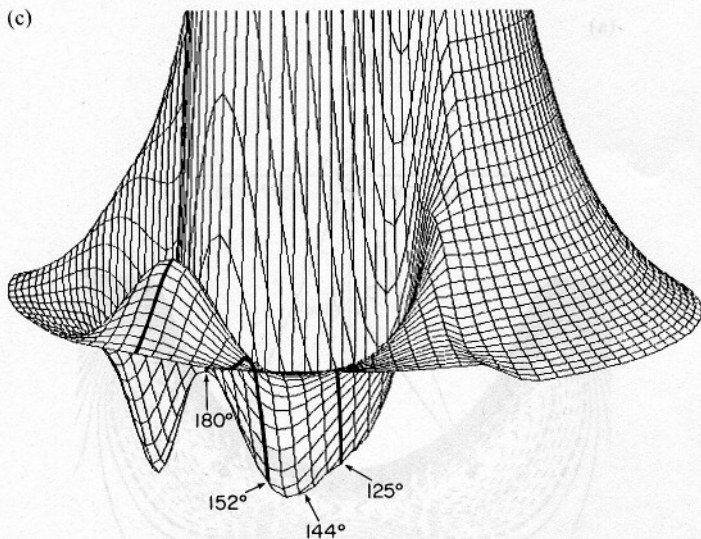


Figure 1. (Continued from previous page.)

metastable predissociating states (trapped by the barrier) and another range of ν_2 values belonging to directly dissociating states. Of course, very low ν_2 values can also yield bound $\nu_1\nu_2$ levels.

Although the above qualitative discussion is predicted on the approximation that ν_1 and ν_2 motion can be thought of as separable, it formed the basis of our analysis in ref. 2 of the MS experimental data on HCN and DCN.* In fact, our estimates [2] of the rates of H or D tunneling through the radial barriers described above allowed us to rationalize the *relative* rates of predissociation of the various $\nu_1\nu_2$ levels. We could not at that time, however, estimate the absolute rates of tunneling very accurately. As we shall demonstrate shortly, the fact that we could explain the MS data in terms of a tunneling model was merely fortuitous. Tunneling actually has little to do with the dynamics of this system.

3. The Need for Dynamical Study

Although the above-outlined interpretation of the MS data in terms of our energy surface seemed quite satisfactory, we had doubts as to whether tunneling through the radial barrier was the dominant predissociation mechanism. After all, it is also possible that intramolecular intermode energy transfer could cause dissociation. That is, ν_1 motion could be trapped behind a barrier (for large ν_2) until $\nu_2 \rightarrow \nu_1$ energy flow occurs, upon which the barrier is lower and the ν_1 energy lies above the barrier. Unfortunately, the time resolution of the MS PFE experiments was not adequate [1] to determine whether the observed H(D)

* The potential energy surfaces are, of course, identical for these two isotopes. Only the vibrational energy levels and tunneling rates differ.

isotope effects could be uniquely attributed to tunneling rather than to different ν_1 and ν_2 energy levels and energy transfer rates.

In an attempt to examine the relative roles of tunneling and intramolecular energy transfer, we undertook a series of classical trajectory calculations aimed at simulating the dissociation of various $\nu_1\nu_2$ levels of HCN and DCN. In this work, we made use of our *ab initio* potential energy surface described in ref. 2. Because of its lower ν_1 and ν_2 frequencies, DCN has many more $\nu_1\nu_2$ levels which show predissociative behavior (i.e., structured PFE spectrum [1]). Hence, we choose to present here the results of our work on DCN and to simply comment on our analogous findings for HCN.

4. Overview of Methods Used

A. Initial Coordinates and Momenta

To simulate the behavior of any $\nu_1\nu_2$ level, we ran 10,000 classical trajectories whose initial D-atom relative coordinates (r, θ) and momenta (p_r, p_θ) were distributed to mimic the probability amplitudes* for radial and angular motion in DCN. To generate the angular wavefunctions, we first followed the position of the radial minimum [$r_{\min}(\theta)$] in the potential surface as a function of θ . The energy along this "path" was used to *define* an angular potential energy. By then numerically integrating the angular Schrödinger equation for this potential we arrived at a set of angular wavefunctions† $X_{\nu_2}(\theta)$ and energies ϵ_{ν_2} . The latter were in remarkably good agreement with the experimentally observed ν_2 energy spacings [1], thereby lending support to the use of approximate separation of angular and radial motions in generating the probability distributions for initial coordinates (θ, r). To obtain the radial vibrational wavefunctions, we proceeded as follows. At each of more than 50 angles (θ), we numerically integrated the radial Schrödinger equation (for fixed θ) to compute $X_{\nu_1}(r)$. The energies along this ν_1 mode were constrained to be those obtained in the MS experiment.

Given the angular wavefunctions, we used $|X_{\nu_2}(\theta)|^2$ as the relative probability weighting for choosing initial θ values in our classical trajectory work. Likewise, $r|X_{\nu_1}(r)|^2$ gave the weighting to attach to any initial r coordinate. (The quantity r comes from the volume element.) The initial momenta p_θ, p_r were obtained

* Admittedly, the predissociating states being studied here are *not* stationary states. However, those levels $\nu_1\nu_2$ which have lifetimes long enough to give rise to structure in the HCN absorption spectrum should be reasonably described as localized wavefunctions in the region of the attractive potential energy well.

† In integrating the angular Schrödinger equation, we had to choose a *fixed* value of the radial coordinate (which enters into the kinetic energy as $p_\theta^2/2\mu r^2$). Since the value of r varied little along the path defining the angular potential, we felt safe in making the assumption that r was constant. Without this approximation we could not have solved for the angular and radial wavefunctions in such a "separated" manner. We would have had to deal with the formidable problem of solving for the coupled (θ, r) vibrational wavefunctions. The fact that the MS absorption spectrum showed reasonable regularity in the energy spacings of the ν_1 and ν_2 modes gave us reasonable confidence that such an approximate separability *ansatz* was not totally in error.

(to within a \pm sign, which was randomly chosen) via energy conservation [e.g., $\epsilon_{v_1} = p_r^2/2\mu + E(r, \theta)$].

B. Integration of Classical Trajectories

For any v_1v_2 level, 10,000 $(\theta, r, p_\theta, p_r)$ initial values were obtained via the above-outlined procedure. Using a time step* of ca. 2×10^{-16} s, and a Gear sixth-order hybrid predictor-corrector numerical integration method [3], the classical equations of motion (including molecular rotation†) were integrated. From the shape of the potential energy surface shown in Figure 1, we knew that once r reached 4.4 a.u. the molecule was on its way to fragmentation if the total energy was above the dissociation limit and p_r was greater than zero. Hence $r > 4.4$ a.u. and $p_r > 0$ was used as our definition of when dissociation had occurred. Although we have indeed included the effects of overall molecular rotation in our classical trajectory simulations, we found no noticeable (on the scale of Fig. 2) influence of the centrifugal forces that arise from such rotations. Clearly, such centrifugal distortions exist but they seem to have little effect for those DCN rotational levels which are populated at ca. 300 K.

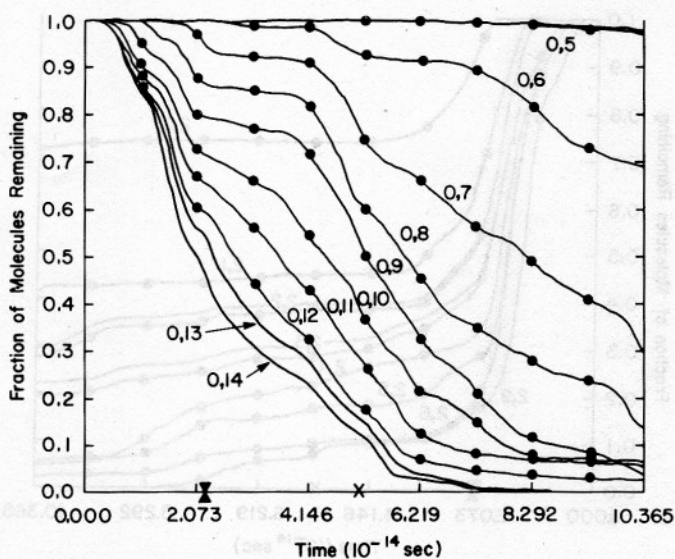
To estimate the contributions to the dissociation rate made by tunneling, we employed a simple WKB approximation to the tunneling probability each time the trapping barrier caused p_r to pass through zero. The height and thickness of the barrier through which tunneling was allowed to occur were estimated by following the *ab initio* surface *radially*‡ from where p_r reached zero, "through" the barrier, to the larger r value where classical motion would again become possible. By employing even this simple tunneling estimate, we were able to examine the fate of each classical trajectory both in the absence and in the presence of tunneling.

As a result of monitoring 10,000 classical trajectories for each v_1v_2 combination, we know what fraction of the trajectories did not dissociate before time t (with and without tunneling). We can thus construct graphs of this fraction as a function of time for each v_1v_2 level. The results of our DCN classical trajectory simulations are presented for $v_1 = 0, 1, 2, 3$ in Figure 2.

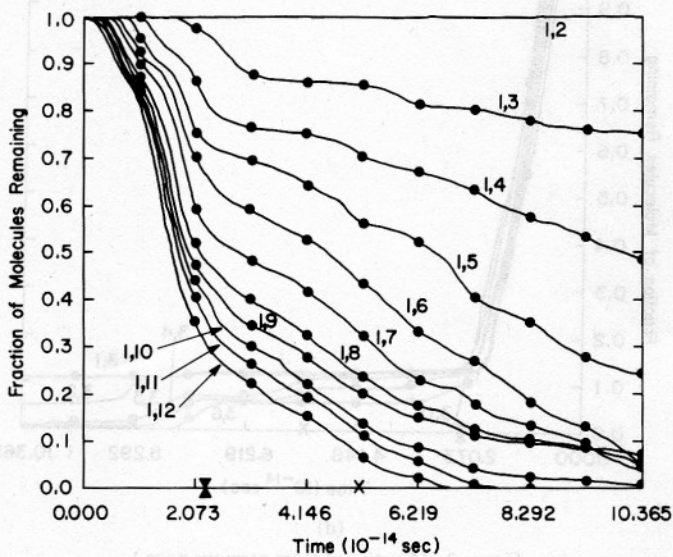
* This time step was arrived at after much experimentation. We wanted to take a small enough step to guarantee that even our longest-lived trajectories could be "turned around" (i.e., run in reverse) to regenerate the same classical path. This time-reversed stability is a test both of the accuracy of our numerical integration routine and of the propriety of our time step. We feel confident that this time step is short enough to guarantee this kind of stability.

† Although we initially explored the effects of populating various rotational states of the DCN molecule, we soon found that rotational motions likely to be populated at 300 K had little effect on the predissociation rates of any of the levels v_1v_2 we simulated. Therefore, in Fig. 2 we present our results for the dissociative rates in which only the one most probably populated (at 300 K) rotational level of DCN is employed.

‡ This is, of course, approximation since the D atom's motion may have had some angular component when it "struck" the barrier. However, because we observed little tunneling contribution to the predissociation rates of HCN or DCN, we feel that this crude approximation does not need to be improved upon. If tunneling were substantial, we would have to treat it more accurately.

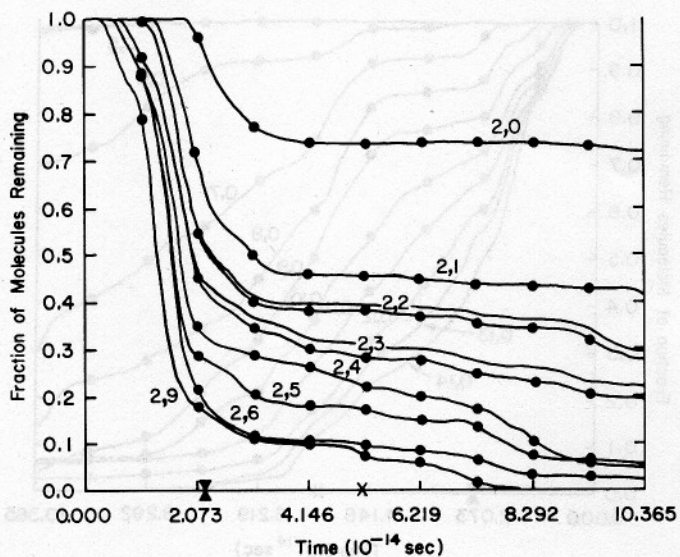


(a)

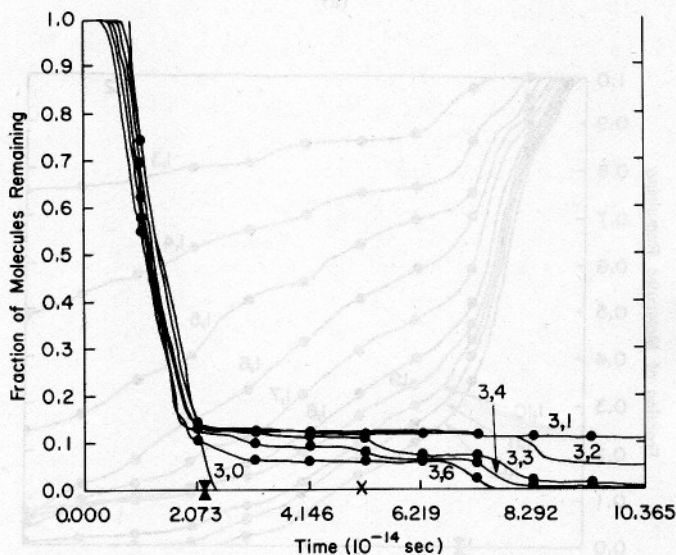


(b)

Figure 2. (a)–(d) give the fraction of molecules that remain undissociated as a function of time. Each integer pair label indicate the particular quantum numbers ν_1, ν_2 . The data are arranged to show the effects of increasing ν_2 at constant ν_1 . On the time axis we included reference markers which indicate the DCN stretching (∇) and bending periods (\times). The rotational period of DCN is approximately 20×10^{-14} s.



(c)



(d)

Figure 2. (Continued from previous page.)

5. Discussion of Results

Clearly for $\nu_1 = 3$ a significant fraction (80–90%) of the DCN molecules dissociate within one bending vibrational period and certainly within a fraction of a rotational period. Hence all ν_2 levels of $\nu_1 = 3$ DCN are expected to give rise to broadened PFE and absorption spectra and appreciable retention of polarization.

The fact that *any* significant fraction of the $\nu_1 = 3$ DCN molecules remain undissociated beyond one bending vibrational period is somewhat surprising since all $\nu_1 = 3$ levels have enough energy to directly dissociate. We take the fact that 0–10% of the molecules do not undergo direct dissociation as an indication that $\nu_1 \rightarrow \nu_2$ intramolecular energy transfer is taking place. This can happen if, as the stretching motion along r is occurring, the DCN also bends so as to produce a radial barrier which the D atom strikes. By hitting this barrier, which Figure 1 shows to be highly curved (i.e., θ dependent), the DCN can convert radial motion (of which it has excess for $\nu_1 = 3$) into angular motion. This lowers the radial kinetic energy and hence “delays” the DCN’s fragmentation.

Unlike the situation for $\nu_1 = 3$ DCN, where we postulate $\nu_1 \rightarrow \nu_2$ energy flow to occur, $\nu_1 = 0,1,2$ DCN seems to show some $\nu_2 \rightarrow \nu_1$ energy transfer. For low ν_2 excitation, the energy in the ν_1 mode lies below the dissociation threshold. As ν_2 is increasingly excited [see Figs. 2(a)–2(c)], the DCN motion begins to sample regions of the surface which have barriers *and* shallower energy minima (along r). Hence radial motion can remain trapped behind the barrier for some time. However, if $\nu_2 \rightarrow \nu_1$ energy transfer takes place, the DCN motion returns to the angular regions of the surface having little or no barrier but now with increased radial kinetic energy. With the newly acquired radial energy the molecule can then dissociate. The reason that $\nu_2 \rightarrow \nu_1$ energy flow seems to occur for $\nu_1 = 0,1,2$ whereas some $\nu_1 \rightarrow \nu_2$ flow occurs for $\nu_1 = 3$ is probably simply a matter of which mode has more energy. When $\nu_1 = 0,1,2$ and $\nu_2 \gtrsim 5$ the bending mode has more energy; for $\nu_1 = 3$ the situation is reversed.

In Figure 2(a) and 2(c) the results for $\nu_1\nu_2 = (0,5)$, $(2,2)$, and $(2,3)$ are shown as double lines. In each case, the lower line gives the results when tunneling was included, as discussed earlier. The upper line relates to our trajectory results in the absence of tunneling. Similarly, very small tunneling contributions were observed for *all* $\nu_1\nu_2$ combinations for DCN and even (although somewhat larger) for HCN. In Figure 2 these tunneling/nontunneling comparisons were not shown for all $\nu_1\nu_2$ levels simply to avoid confusion in the graphs. Our conclusion, therefore, is that tunneling is not appreciable.

Although there does seem to be some energy transfer between the ν_1 and ν_2 modes, our simulated rates of dissociation retain substantial mode specificity. For example, levels $(\nu_1, \nu_2) = (0,5)$ and $(1,3)$ show markedly different decay although they have nearly (within ca. 130 cm^{-1}) the same total energy. Likewise levels $(0,10)$, $(2,5)$, and $(3,3)$ which have common energies within 130 cm^{-1} , show very different decay kinetics. DCN and HCN thus can be said to display mode specificity within the time scale of our simulations.

6. Summary

The data obtained in our classical trajectory simulations of the predissociation of various $\nu_1\nu_2$ levels of DCN do indeed help interpret the MS experimental PFE spectra of HCN and DCN. Moreover, they provide insight into the mechanism of the fast (i.e., essentially direct) and slower ($\nu_2 \rightarrow \nu_1$ transfer) predissociation

steps. It seems that intramolecular energy transfer, rather than tunneling, plays the central role.

There are, however, some points that remain to be addressed. Although our *ab initio* potential energy surface seems to give an excellent line-by-line [except for $\nu_1 = 2$ DCN (see ref. 2)] interpretation of the PFE spectra, the absolute rates of predissociation obtained in our trajectory work seem to be a little too fast for certain $\nu_1 = 0, 1$ levels. For example, we claim that ca. 50% of the $\nu_1 = 1, \nu_2 = 4$ DCN molecules should predissociate within a rotational period. MS had to infer the existence of $\nu_1 = 1, \nu_2 = 4$ predissociation from their absorption spectrum and from the fact that this level certainly has enough total energy to lie above the dissociation threshold.

A few small discrepancies such as that mentioned above make us wonder about the use of *classical* trajectories in studying intramolecular energy transfer. After all, arbitrary amounts of energy can be transferred among the ν_1 and ν_2 modes within classical mechanics. The phase relationships of the angular and radial parts of the vibrational wavefunctions limit energy transfer in quantum mechanics. Moreover, the local deBroglie wavelengths corresponding to the radial and angular degrees of freedom are certainly *not* small compared with distances over which the potential energy surface varies. Hence, there seems to be little that leads one to expect that a classical treatment of the D(H) atom's motion should be valid. Therefore, it is useful to ask why our classical treatment was able to do so well in describing trends in the rates of predissociation of DCN. For this reason, we are now beginning to explore exactly this same predissociation problem using the quantum mechanical tools previously used in our laboratory [4] to explore the rates of predissociation of triatomic van der Waals complexes. The comparison of the results of these quantum studies with those of the present classical trajectory investigation will be most interesting and important.

Acknowledgments

This work was supported by the National Science Foundation through Grant No. 7906645 and through their support of the Utah DEC 2060 computer facility.

Bibliography

- [1] M. T. MacPherson and J. P. Simons, *J. Chem. Soc. Faraday II* **74**, 1965 (1978).
- [2] D. T. Chuljian and J. Simons, *J. Am. Chem. Soc.* **104**, 645 (1982).
- [3] C. W. Gear, *SIAM J. Num. Anal.* **213**, 69 (1965).
- [4] Z. Bacić and J. Simons, *Int. J. Quantum Chem. Quantum Chem. Symp.* **14**, 467 (1980); *J. Phys. Chem.* **86**, 1192 (1982).

Received March 31, 1982